ISSN: 2178-7727

AI-Powered X-ray System for Detecting Tuberculosis, Pneumonia and COVID-19

Rashmi N, Mamatha K R, Thejaswini S, Dr. Girish H

Dept. of ECE, B M S Institute of Technology and Management Bengaluru, Karnataka, India
Dept. of ECE, B M S Institute of Technology and Management Bengaluru, Karnataka, India.
Dept. of ETE, B M S Institute of Technology and Management Bengaluru, Karnataka, India
Professor, Department of ECE, Cambridge Institute of Technology, Bangalore

ABSTRACT

In rural areas, the availability of radiologists is limited, and the diagnostic process for them can be challenging due to the high volume of patients at the same clinic. To address this issue and reduce the time required for diagnosis, a robust technology for chest X-ray image analysis has been introduced. This paper presents two convolutional neural network (CNN) models designed for multi-class classification of diseases such as Tuberculosis, Pneumonia, and COVID-19. The authors performed image pre-processing, data augmentation, and employed deep learning techniques to classify chest X-ray (CXR) images, using a dataset of 18,781 images obtained from Kaggle. The data was split into training, validation, and test sets in an 80:15:5 ratio. The system is designed to assign a probability to each diagnosis, generate a simple report, and eliminate the delay in report analysis. CNNs and a medical AI library were used to develop the models. Testing results showed that Model 1 achieved accuracy rates of 94.5%, 99.3%, 99.5%, and 94.9% for Normal, Tuberculosis, Pneumonia, and COVID-19 classes, respectively, with sensitivity values of 96.7%, 82.9%, 100%, and 86.9%. Model 2 achieved accuracy rates of 95.1%, 99.2%, 99.3%, and 94.8% for the same classes. The proposed models have the potential for automated and expedited diagnosis of these diseases.

KEYWORDS: Convolution neural network, image augmentation, multi-class classification, medical ai

INTRODUCTION

As the population continues to grow, the demand for medical care is increasing, and thoracic disorders are becoming more prevalent. In India, there is a significant disparity in the availability of radiologists, with one radiologist for every 100,000 people compared to the United States, where the ratio is 1:10,000. This shortage is particularly problematic in rural areas, where limited access to radiologists often delays diagnosis and treatment. Factors such as rising incomes, increased insurance coverage, a higher incidence of chronic illnesses, and an aging population are driving the demand for healthcare across India.

Tuberculosis remains a major public health issue in India, with an estimated 220,000 deaths annually and about a quarter of the world's tuberculosis cases occurring in the country. In March 2017, the Government of India set a goal to eliminate tuberculosis by 2025. Similarly, COVID-19, caused by the coronavirus, has led to severe acute respiratory syndrome and numerous deaths. Chest X-rays are crucial in detecting COVID-19, and prompt treatment is essential.

Pneumonia, a lung infection where fluid or pus fills the air sacs of one or both lungs, causing inflammation, can also be diagnosed efficiently using X-rays. X-rays are a cost-effective and reliable method for diagnosing various illnesses by creating images of tissues and bones through radioactive electromagnetic waves. Typically, radiologists interpret these X-ray images to ensure accurate diagnosis. However, the global shortage of radiologists often leads to delayed diagnoses and unnecessary fatalities.

Image processing, which enhances or extracts information from images, is vital in this context. Convolutional Neural Networks (CNNs) have emerged as one of the most effective deep learning techniques in medical imaging, particularly for their ability to automatically learn features from domain-specific images. This research aims to develop a deep learning-based automated X-ray screening method that classifies chest X-ray

ISSN: 2178-7727

images into four categories: normal, tuberculosis, pneumonia, and COVID-19. The model assigns a probability score to each class.

The rest of the paper is organized as follows: Section II provides background information, Section III introduces the proposed dataset, Section IV covers data preparation, Section V details the methodology used, Section VI presents the results and discusses various metrics, and Section VII concludes the paper and outlines future work..

BACKGROUND

Extensive research has been conducted on disease diagnosis using chest X-ray images. For instance, Ref. [1] proposed a method to address uncertainty in chest X-ray analysis by incorporating dropout layers in fully connected layers, with the second of the three architectures achieving the highest accuracy at 96.44%. Ref. [2] utilized the pre-trained Xception model to classify 14 different thoracic diseases, achieving an overall accuracy of 88.6%, with the Hernia class having the highest AUC (Area Under Curve) value. Ref. [3] introduced a framework called DeTraC (Decomposition, Transfer Learning, and Class Composition) and applied transfer learning to several models (AlexNet, VGG, GoogleNet, ResNet), with ResNet achieving the highest accuracy of 99.8%. Ref. [4] employed transfer learning on DenseNet121 to classify six broad categories of thoracic diseases, achieving over 90% accuracy in three of those categories. Finally, Ref. [5] recommended segmenting the lung area before focusing on that segmented region to extract features for disease prediction from chest X-ray images.

DATASET

The system utilizes three distinct datasets for CXR images related to tuberculosis, pneumonia, and COVID-19:

Tuberculosis (TB) Chest X-ray Database: Available on Kaggle, this dataset includes images from the Montgomery and Shenzhen datasets, the Belarus dataset, and the NIAID TB dataset. The Montgomery County and Shenzhen datasets, provided by the U.S. National Library of Medicine (NLM), contain posterior-anterior chest X-ray images with 138 images in Montgomery and 667 in Shenzhen. Montgomery images have resolutions of either 4020x4892 or 4892x4020 pixels, while Shenzhen images have a variable resolution of approximately 3000x3000 pixels. Of the 138 Montgomery images, 58 are tuberculosis-affected, and 80 are normal. In the Shenzhen dataset, 336 of 662 images are tuberculosis-affected, while 324 are normal, resulting in 394 TB-infected and 406 normal chest X-ray images in the NLM database, all in PNG format. Additionally, the Kaggle TB Chest X-ray Database contains 3,500 normal and 700 tuberculosis-affected chest X-ray images in JPEG format.

Kaggle Chest X-Ray Images (Pneumonia): This dataset contains 5,856 JPEG images, divided into three directories: test, train, and validate. Among these, 1,583 images are of normal chest X-rays, while 4,273 images depict pneumonia-affected chest X-rays.

COVID-19 Radiology Database: Collected from the Kaggle COVID-19 radiology database, this dataset includes four directories and five files, with two primary directories being used: COVID and Normal. The COVID directory contains 3,616 JPEG images of chest X-rays identified as COVID positive, while the Normal directory contains 10,198 JPEG images of chest X-rays not identified as COVID positive.

DATA PREPARATION

This process involves converting images to a uniform format and generating a CSV file:

Removing Data Redundancy: Since many images in the datasets were similar and overlapped, duplicate images were excluded to prevent redundancy. This approach led to an accuracy of 98.6%, which was higher than the 96.62% achieved by direct classification.

DOI: https://doi.org/10.57030/ASCI.25.4.AS27

ISSN: 2178-7727

Augmentation: Normalization was applied to both the training and validation set images. Additionally, random-sized cropping was introduced to the training data images to enhance model performance.

Image Conversion: To ensure all classification data was in a consistent format, images in the tuberculosis, pneumonia, and COVID datasets that were originally in PNG format were converted to JPEG.

CSV File Creation: For multiclass classification and compatibility with the Medical AI library, the data was required to be in a one-hot encoded vector format, necessitating the creation of a CSV file, as illustrated in Table II.

METHODOLOGY

CNNs are utilized to develop classification models. As a Deep Learning-based approach, CNNs have gained popularity in image classification tasks due to their remarkable results. Their widespread use is largely attributed to their ability to automatically learn features from the input images. Unlike traditional feed-forward networks, CNNs.

TABLE I
DATA USED FROM CONSIDERED DATASET

Category	***Tuberculosis (TB) Chest X-ray Database***	***Chest X-Ray Images (Pneumonia)***	***COVID19 radiology database***
Tuberculosis	700		
Pneumonia		4273	
Normal			10198
Covid			3636

TABLE II
CSV FILE FOR MULTICLASS CLASSIFICATION

Category	***Normal***	***Tuberculosis***	***Pneumonia***	***Covid***
Normal-5126.jpeg	1	0	0	0
Normal-6597.jpeg	1	0	0	0
…	…	…	…	…
person1078 bacteria 3018.jpeg person693 bacteria 2590.jpeg	0 0	0 0	0 0	1 1
person1541 virus 2681.jpeg	0	0	0	1

CNNs optimize tasks with a significantly smaller number of parameters by retaining essential features and patterns or identification, while filtering out irrelevant variations during classification tasks.

DOI: https://doi.org/10.57030/ASCI.25.4.AS27

ISSN: 2178-7727

Model 1 Architecture		
Layer No.	Layer type - size	Activation function
1	Convol_1 - 3x3x32	ReLu
2	Max_pooling_1 - 2x2	-
3	Convol_2 - 3x3x64	ReLu
4	Max_pooling_2 - 2x2	-
5	Convol_3 - 3x3x128	ReLu
6	Max_pooling_3 - 2x2	-
7	Convol_4 - 3x3x256	ReLu
8	Max_pooling_4 - 2x2	-
9	Convol_5 - 3x3x256	ReLu
10	Max_pooling_5 - 2x2	-
11	global_average_pooling_1	-
12	flatten	-
13	Dense_1 - 512	ReLu
14	dropout	-
15	dense_2	Sigmoid

Fig. 1. Description of CNN architecture of the proposed model1

The architecture of Model 1, as illustrated in Fig. 1, includes 5 alternating convolutional and pooling layers, followed by a global average pooling layer before reaching the fully connected layers. The fully connected section features a single dense layer, succeeded by a dropout layer with a 20% dropout rate to prevent overfitting and enhance model robustness. The model was trained for 10 epochs with a batch size of 32 images, using callbacks to mitigate overfitting. It achieved a training accuracy of 96.27% and a validation accuracy of 95.42%, with training and validation losses of 0.0501 and 0.0608, respectively.

Model 2 Architecture		
Layer No.	Layer type - size	Activation function
1	Convol_1 - 3x3x32	ReLu
2	Max_pooling_1 - 2x2	-
3	Convol_2 - 3x3x64	ReLu
4	Max_pooling_2 - 2x2	-
5	Convol_3 - 3x3x128	ReLu
6	Max_pooling_3 - 2x2	-
7	Convol_4 - 3x3x256	ReLu
8	Max_pooling_4 - 2x2	-
9	Convol_5 - 3x3x512	ReLu
10	Max_pooling_5 - 2x2	-
11	global_average_pooling_1	-
12	flatten	-
13	dropout_1	-
14	Dense_1 - 512	ReLu
15	dropout_2	-
16	dense_2	Sigmoid

Fig. 2. Description of CNN architecture of the proposed model2

ISSN: 2178-7727

The architecture of Model 2, as shown in Fig. 2, comprises 5 alternating convolutional and pooling layers, followed by a global average pooling layer and an additional dropout layer with a 20% dropout rate before the fully connected layers. The fully connected section includes a single dense layer, succeeded by another dropout layer with a 20% probability to reduce overfitting and enhance model robustness. This model was trained for 11 epochs with a batch size of 32 images, employing callbacks to mitigate overfitting. It achieved a training accuracy of 96.39% and a validation accuracy of 95.32%, with training and validation losses of 0.0496 and 0.0605, respectively.

RESULTS AND DISCUSSIONS

A.Training Graph Analysis

After training graphs were plotted for training and validation accuracy and training and validation loss to check for overfitting.

Fig. 3. Accuracy and loss plots for model 1

Fig. 3 shows no signs of overfitting in case of model 1.

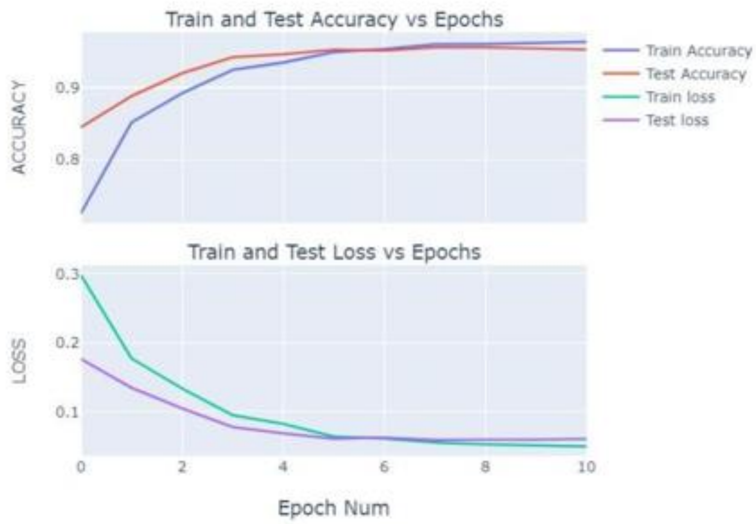

Fig. 4. Accuracy and loss plots for model 2

ISSN: 2178-7727

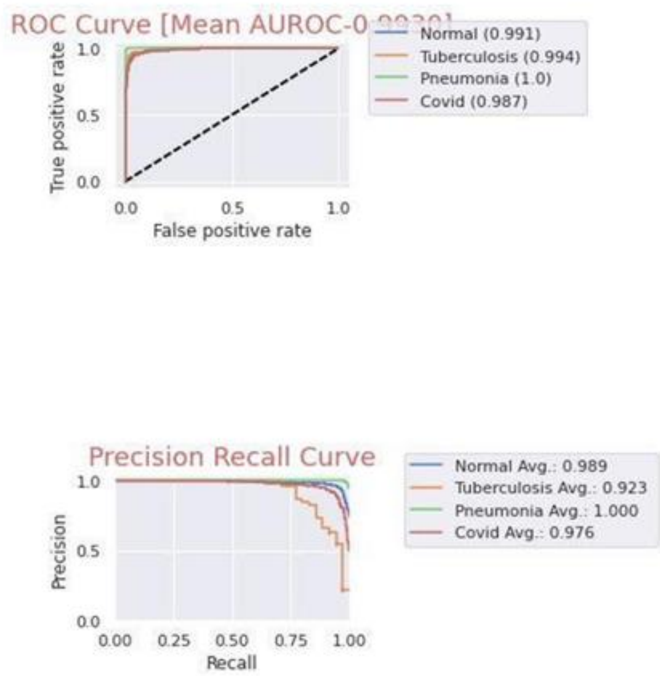

Fig. 4 shows no signs of overfitting in case of model 2.

B. Receiver Operating Characteristic (ROC) and Precision- Recall curves

Based on a ROC curve, an analysis shows the trade off between sensitivity (TPR) and specificity. The curves for both the models (as shown in Fig. 5 and Fig. 6) are closer to the top left corners indicating a promising and fair accuracy.

For various sample thresholds, precision-recall curves show the difference between precision and recall. A high AUC (area under the curve) value represents a high recall and a high precision. The high precision value reflects a low rate for false positives, and high recall reflects a low rate for false negatives.

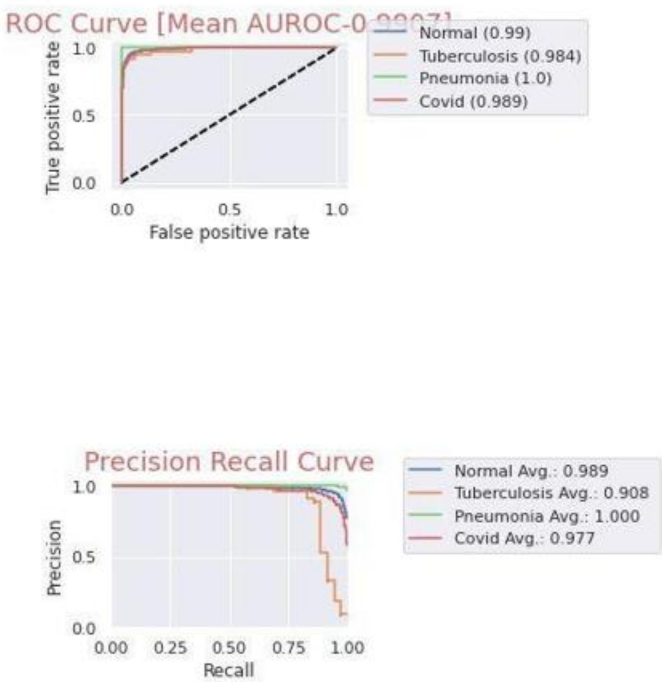

Fig. 5. ROC and precision recall curves for model 1

ISSN: 2178-7727

Sensitivity, Specificity and Individual Class Accuracy Anal-ysis

A sensitivity (True Positive rate) specifies the proportion of those who have a condition (affected) that can be properly identified for that condition. A specificity rate (True Negative rate) specifies those who do not have the condition (unaffected) and are correctly identified as such.

Model Sensitivity and Specificity Details (Th=0.5)

	Sensitivity	Specificity	PPV	NPV	AUC	F1
Normal	0.967	0.926	0.92	0.97	0.947	0.943
Tuberculosis	0.829	0.998	0.935	0.994	0.913	0.879
Pneumonia	1.0	0.993	0.973	1.0	0.997	0.986
Covid	0.869	0.984	0.961	0.944	0.927	0.913

Validation Accuracy Details (Th=0.5)

	TP	TN	FP	FN	Accuracy	Prevalence
Normal	492	542	43	17	0.945	0.465
Tuberculosis	29	1057	2	6	0.993	0.032
Pneumonia	213	875	6	0	0.995	0.195
Covid	293	745	12	44	0.949	0.308

Fig. 7. Sensitivity, specificity and accuracy values for individual classes

Fig. 7 shows the sensitivity, specificity and accuracy metrics for model 1. For classes normal, tuberculosis, pneumonia and covid the sensitivity values are 96.7%, 82.9%, 100% and 86.9% respectively, the specificity values are 92.6%, 99.8%, 99.3% and 98.4% respectively and accuracy's are 94.5%, 99.3%, 99.5% and 94.9% respectively.

Model Sensitivity and Specificity Details (Th=0.5)

	Sensitivity	Specificity	PPV	NPV	AUC	F1
Normal	0.972	0.932	0.925	0.975	0.952	0.948
Tuberculosis	0.771	0.999	0.964	0.992	0.885	0.857
Pneumonia	0.995	0.992	0.968	0.999	0.994	0.981
Covid	0.869	0.983	0.958	0.944	0.926	0.911

Validation Accuracy Details (Th=0.5)

	TP	TN	FP	FN	Accuracy	Prevalence
Normal	495	545	40	14	0.951	0.465
Tuberculosis	27	1058	1	8	0.992	0.032
Pneumonia	212	874	7	1	0.993	0.195
Covid	293	744	13	44	0.948	0.308

Fig. 8. Sensitivity, specificity and accuracy values for individual classes

Fig. 8 shows the sensitivity, specificity and accuracy metrics for model 2. For classes normal, tuberculosis, pneumonia and covid the sensitivity values are 97.2%, 77.1%, 99.5% and 86.9% respectively, the specificity values are 93.2%, 99.9%, 99.2% and 98.3% respectively and accuracy's are 95.1%, 99.2%, 99.3% and 94.8% respectively.

C. Grad-CAM analysis

Grad-CAM (Gradient-weighted Class Activation Mapping) is a technique used to generate "visual explanations" for classifier performance in CNN-based models. It works by integrating the gradients of any target concept into the final classifier, providing a coarse localization map that highlights the key areas in the image relevant for predicting that concept. This method enhances the transparency of various CNN model

DOI: https://doi.org/10.57030/ASCI.25.4.AS27

families and can be applied across a wide range of them.

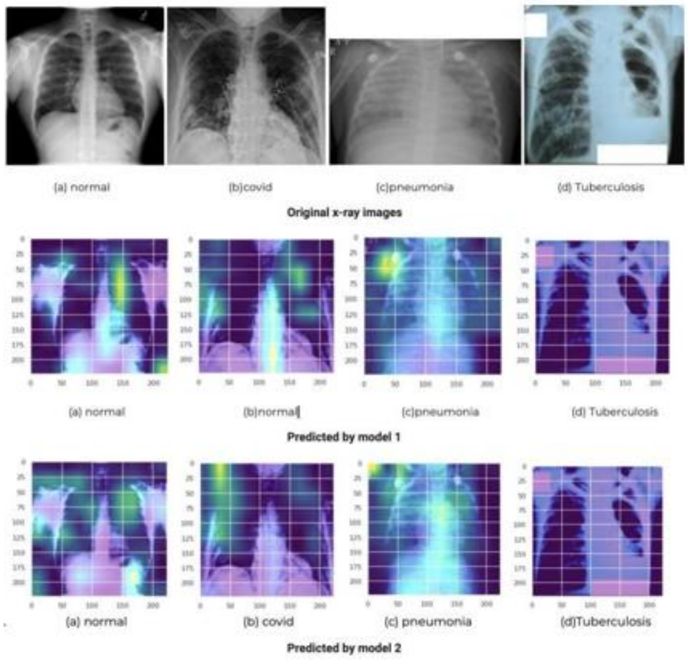

Fig. 9. Grad-CAM results of predictions my model 1 and model 2

The Grad-CAM results highlight the regions of interest that the models focus on when predicting a sample image. As illustrated in Fig. 9, Model 1 incorrectly classified a COVID-19 sample as normal. To minimize such misclassifications in the future, the model's accuracy can be further enhanced.

CONCLUSION AND FUTURE WORK

The authors developed a deep learning model using a deep convolutional neural network (CNN) architecture to diagnose chest diseases like pneumonia, tuberculosis, and COVID-19 from X-ray images. They compared the performance of two proposed CNN models in classifying tuberculosis, pneumonia, COVID-19, and normal chest X-ray images, achieving accuracies of 96.27% and 96.39%, respectively, with model loss reaching an acceptable level in terms of performance. Grad-CAM was used to visualize lung segmentation, confirming that critical segments for assessing a patient’s lung condition were accurately considered. Such an advanced diagnostic tool has the potential to save many lives by reducing delays or inaccuracies in diagnosis. To further enhance accuracy, the number of chest X-ray images used for model training could be increased. Additionally, segmentation and localization techniques could be employed to better illustrate the basis for predictions. In the future, this model could also be adapted to detect conditions in MRIs and mammograms.

REFERENCES

[1] G. Eason, B. Noble, and I. N. Sneddon, “On certain integrals of Lipschitz-Hankel type involving products of Bessel functions,” Phil. Trans. Roy. Soc. London, vol. A247, pp. 529–551, April 1955. (references) M. Sardogan, A. Tuncer and Y. Ozen, "Plant Leaf Disease Detection and Classification Based on CNN with LVQ Algorithm," 2018 3rd International Conference on Computer Science and Engineering (UBMK), 2018, pp. 382-385.

[2] D. Bini, D. Pamela and S. Prince, "Machine Vision and Machine Learning for Intelligent Agrobots: A review" 2020 5th International Conference on Devices, Circuits and Systems (ICDCS), 2020, pp. 12- 16.

[3] G. M. Sharif Ullah Al- Mamun et al., "Performance Analysis of Multipurpose AGROBOT," 2019 IEEE International WIE Conference on Electrical and Computer Engineering (WIECON-ECE), 2019, pp. 1-4.

[4] H Durmuş, E. O. Güneş, M. Kırcı and B. B. Üstündağ, "The design of general purpose autonomous agricultural mobile-robot: “AGROBOT”," 2015 Fourth International Conference on Agro- Geoinformatics

(Agro- geoinformatics),2015,pp.49-53.
[5] N G. Kurale and M. V. Vaidya, "Classification of Leaf Disease Using Texture Feature and Neural Network Classifier," 2018 International Conference on Inventive Research in Computing Applications (ICIRCA),2018,pp. 1-6.
[6] IoT based home automation using Blynk cloud, J. Chetan Naik, B. S. Deeksha, H. Girish, Gurusharan Kashetty, T. G. Shivapanchakshari, Manohar Sai Polakam, Journal: AIP Conference Proceedings, AIP Conf. Proc. 2965, 020006 (2024), https://doi.org/10.1063/5.0215427, Published: July 2024
[7] IoT based fire alarm system using Blynk app, T. Bhargava, H. Kishor Kumar, Pramod Mahalingappa Godi, H. Girish, J. Chetan Naik, Journal: AIP Conference Proceedings, AIP Conf. Proc. 2965, 020007 (2024), https://doi.org/10.1063/5.0212325, Published: July 2024
[8] Dr. GIRISH H et. al., “Design and Analysis of a Machine learning based Agriculture bot”, Tuijin Jishu/Journal of Propulsion Technology ISSN: 1001-4055 Vol. 44 No. 6 (2023)
[9] Dr. GIRISH H et. al., “Integrating Disaster Data Clustering with Neural Networks for Comprehensive Analysis”, Tuijin Jishu/Journal of Propulsion Technology ISSN: 1001-4055 Vol. 45 No.1 (2024).
[10] Dr. GIRISH H et. al., “ROBOTIC INNOVATION IN E-DELIVERY SYSTEMS: A DESIGN AND MODELING APPROACH”, The Seybold report ISSN 1533-9211, 2023.
[11] Dr. GIRISH H et. al., “Machine Learning based Agriculture Bot”, International Conference on Smart Technologies, Communication and Robotics [ICSCR-2023] in association with IJSRSET Print ISSN: 2395-1990 | Online ISSN : 2394-4099 (www.ijsrset.com) doi : https://doi.org/10.32628/IJSRSET
[12] Dr. GIRISH H et.al., “A GSM-Based System for Vehicle Collision Detection and Alert”. International Conference on Smart Technologies, Communication and Robotics [ICSCR-2023] in association with IJSRSET Print ISSN: 2395-1990 | Online ISSN : 2394-4099 (www.ijsrset.com) doi : https://doi.org/10.32628/IJSRSET
[13] H. Girish, T. G. Manjunat and A. C. Vikramathithan, "Detection and Alerting Animals in Forest using Artificial Intelligence and IoT," 2022 IEEE Fourth International Conference on Advances in Electronics, Computers and Communications (ICAECC), 2022, pp. 1-5, doi: 10.1109/ICAECC54045.2022.9716679.
[14] A. Devipriya, H. Girish, V. Srinivas, N. Adi Reddy and D. Rajkiran, "RTL Design and Logic Synthesis of Traffic Light Controller for 45nm Technology," 2022 3rd International Conference for Emerging Technology (INCET), 2022, pp. 1-5, doi: 10.1109/INCET54531.2022.9824833.
[15] S. Vaddadi, V. Srinivas, N. A. Reddy, G. H, R. D and A. Devipriya, "Factory Inventory Automation using Industry 4.0 Technologies," 2022 IEEE IAS Global Conference on Emerging Technologies (GlobConET), 2022, pp. 734-738, doi: 10.1109/GlobConET53749.2022.9872416.
[16] T G Manjunath , A C Vikramathithan , H Girish, “Analysis of Total Harmonic Distortion and implementation of Inverter Fault Diagnosis using Artificial Neural Network”, Journal of Physics: Conference Series, Volume 2161, 1st International Conference on Artificial Intelligence, Computational Electronics and Communication System (AICECS 2021) 28-30 October 2021, Manipal, India. https://iopscience.iop.org/issue/1742-6596/2161/1
[17] GIRISH H , “Internet of Things Based Heart Beat Rate Monitoring System”, © September 2022 | IJIRT | Volume 6 Issue 4 | ISSN: 2349-6002 IJIRT 156592 INTERNATIONAL JOURNAL OF INNOVATIVE RESEARCH IN TECHNOLOGY 227
[18] Dr Girish H, Dr. Mangala Gowri , Dr. Keshava Murthy , Chetan Naik J, Autonomous Car Using Deep Learning and Open CV, PAGE NO: 107-115, VOLUME 8 ISSUE 10 2022, Gradiva review journal, ISSN NO : 0363-8057, DOI:10.37897.GRJ.2022.V8I8.22.50332
[19] Girish H. "Intelligent Traffic Tracking System Using Wi-Fi ." International Journal for Scientific Research and Development 8.12 (2021): 86-90.
[20] Girish H, Shashikumar D R, “Emission monitoring system using IOT”, Dogo Rangsang Research Journal, UGC Care Group I Journal, ISSN: 347-7180, Vol – 8 Issue-14, No.6, 2020.
[21] Girish H, Shashikumar D R, “Display and misson computer software loading”, International journal of engineering research & Technology (IJERT), ISSN: 2278-0181, Vol – 10 Issue-08, No.13, August 2020.
[22] Girish H, Shashikumar D R, “A Novel Optimization Framework for Controlling Stabilization Issue in Design Principle of FinFET based SRAM”, International Journal of Electrical and Computer Engineering (IJECE) Vol. 9, No. 5 October 2019, pp. 4027~4034. ISSN: 2088-8708, DOI: 10.11591/ijece.v9i5.pp.4027-

ISSN: 2178-7727

4034
[23] Girish H, Shashikumar D R, “PAOD: a predictive approach for optimization of design in FinFET/SRAM”, International Journal of Electrical and Computer Engineering (IJECE) Vol. 9, No. 2, April 2019, pp. 960~966. ISSN: 2088-8708, DOI: 10.11591/ijece.v9i2.pp.960-966
[24] Girish H, Shashikumar D R, “SOPA: Search Optimization Based Predictive Approach for Design Optimization in FinFET/SRAM”, © Springer International Publishing AG, part of Springer Nature 2019 Silhavy (Ed.): CSOC 2018, AISC 764, pp. 21–29, 2019. https://doi.org/10.1007/978-3-319-91189-2_3.
[25] Girish H, Shashikumar D R, “Cost-Effective Computational Modelling of Fault Tolerant Optimization of FinFET-based SRAM Cells”, © Springer International Publishing AG 2017 R. Silhavy et al. (eds.), Cybernetics and Mathematics Applications in Intelligent Systems, Advances in Intelligent Systems and Computing 574, DOI 10.1007/978-3-319-57264-2_1.
[26] Girish H, Shashikumar D R, “A Survey on the Performance Analysis of FinFET SRAM Cells for Different Technologies”, International Journal of Engineering and Advanced Technology (IJEAT) ISSN: 2249 – 8958, Volume-4 Issue-6, 2016.
[27] Girish H, Shashikumar D R, “Insights of Performance Enhancement Techniques on FinFET-based SRAM Cells”, Communications on Applied Electronics (CAE) – ISSN: 2394-4714, Foundation of Computer Science FCS, New York, USA .Volume 5 – No.6, July 2016 – www.caeaccess.org
[28] Girish H, Shashikumar D R, “DESIGN OF FINFET”, International Journal of Engineering Research ISSN: 2319-6890) (online), 2347-5013(print) Volume No.5 Issue: Special 5, pp: 992-1128, doi: 10.17950/ijer/v5i5/013 2016.
[29] Dr. MANGALA GOWRI S G, Dr. SHASHIDHAR T M, Dr. SUNITHA R, SHYLAJA V, Dr. GIRISH H, “DESIGN OF 3-BIT CMOS WALLACE MULTIPLIER” , Seybold report, ISSN 1533-9211, Volume 18, Page No: 1260-1271 DOI: 10.5281/zenodo.8300481
[30] Dr. Mangala Gowri S G, Dr. Girish H, Ramesh N, Dr. Nataraj Vijaypur, “IOT based plant monitoring system and smart irrigation using new features” ResMilitaris, vol.13, n°2, January Issue 2023 https://resmilitaris.net/menu-script/index.php/resmilitaris/article/view/3312/2608
[31] Girish H.2023, Smart Theft Securityvehicular System Using Iot. Int J Recent Sci Res. 14(02), pp. 2881-2884. DOI: http://dx.doi.org/10.24327/ijrsr.2023.1402.0591
[32] Dr. Mangala Gowri S G, Dr. Girish H, Dr. Santosh Dattatray Bhopale, Weed Detection based on Neural Networks, International Journal of All Research Education and Scientific Methods (IJARESM), ISSN: 2455-6211 Volume 11, Issue 3, March-2023, Impact Factor: 7.429, Available online at: www.ijaresm.com DOI: https://doi.org/11.56025/IJARESM.2023.11323351
[33] Shashidhara, K.S., Girish, H., Parameshwara, M.C., Rai, B.K., Dakulagi, V. (2023). A Novel Approach for Identification of Healthy and Unhealthy Leaves Using Scale Invariant Feature Transform and Shading Histogram-PCA Techniques. In: Shetty, N.R., Patnaik, L.M., Prasad, N.H. (eds) Emerging Research in Computing, Information, Communication and Applications. Lecture Notes in Electrical Engineering, vol 928. Springer, Singapore. https://doi.org/10.1007/978-981-19-5482-5_47